Acta Crystallographica Section F
Structural Biology Communications
ISSN 2053-230X

The structure of lactoferrin-binding protein B from *Neisseria meningitidis* suggests roles in iron acquisition and neutralization of host defences

Cory L. Brooks,[a]* Elena Arutyunova[b] and M. Joanne Lemieux[b]*

[a]Department of Chemistry, California State University Fresno, Fresno, CA 93710, USA, and [b]Department of Biochemistry, University of Alberta, Edmonton, AB T6J 2H7, Canada

Correspondence e-mail: cbrooks@csufresno.edu, mlemieux@ualberta.ca

Received 6 August 2014
Accepted 27 August 2014

PDB reference: LbpB N-lobe, 4uc9

Pathogens have evolved a range of mechanisms to acquire iron from the host during infection. Several Gram-negative pathogens including members of the genera *Neisseria* and *Moraxella* have evolved two-component systems that can extract iron from the host glycoproteins lactoferrin and transferrin. The homologous iron-transport systems consist of a membrane-bound transporter and an accessory lipoprotein. While the mechanism behind iron acquisition from transferrin is well understood, relatively little is known regarding how iron is extracted from lactoferrin. Here, the crystal structure of the N-terminal domain (N-lobe) of the accessory lipoprotein lactoferrin-binding protein B (LbpB) from the pathogen *Neisseria meningitidis* is reported. The structure is highly homologous to the previously determined structures of the accessory lipoprotein transferrin-binding protein B (TbpB) and LbpB from the bovine pathogen *Moraxella bovis*. Docking the LbpB structure with lactoferrin reveals extensive binding interactions with the N1 subdomain of lactoferrin. The nature of the interaction precludes apolactoferrin from binding LbpB, ensuring the specificity of iron-loaded lactoferrin. The specificity of LbpB safeguards proper delivery of iron-bound lactoferrin to the transporter lactoferrin-binding protein A (LbpA). The structure also reveals a possible secondary role for LbpB in protecting the bacteria from host defences. Following proteolytic digestion of lactoferrin, a cationic peptide derived from the N-terminus is released. This peptide, called lactoferricin, exhibits potent antimicrobial effects. The docked model of LbpB with lactoferrin reveals that LbpB interacts extensively with the N-terminal lactoferricin region. This may provide a venue for preventing the production of the peptide by proteolysis, or directly sequestering the peptide, protecting the bacteria from the toxic effects of lactoferricin.

1. Introduction

Bacterial pathogenesis is dependent on the acquisition of nutrients from the environment of the host organism. It has long been recognized that *Neisseria meningitidis* virulence is critically dependent on iron availability (Archibald & DeVoe, 1978). *N. meningitidis* is a principal source of bacterial meningitis in children, and the crucial role of iron acquisition in virulence has generated considerable interest in targeting the protein systems involved in iron transport as vaccine candidates (Rokbi *et al.*, 1997, 2000; Pettersson *et al.*, 2006; Lissolo *et al.*, 1995; Ala'Aldeen & Borriello, 1996; Ala'Aldeen *et al.*, 1994).

During bacterial invasion of the human host, *N. meningitidis* must survive in the oropharynx and bloodstream, environments that contain virtually no free iron for the bacteria to use as a nutrient source. Iron in the human body is primarily stored in iron-binding proteins such as haemoglobin (red blood cells), ferritin (intracellular iron), transferrin (serum and lymph) and lactoferrin (milk, secretions and mucosal surfaces). These iron-binding proteins have extraordinarily high affinities, rendering the effective concentration of free iron in the human fluids to be zero (Weinberg, 2009). While the majority of pathogenic bacteria employ siderophores to chelate and scavenge iron (Weinberg, 2009), *Neisseria* has evolved a series of protein transporters that directly hijack iron sequestered in host transferrin, lactoferrin and haemoglobin (Schryvers & Stojiljkovic,

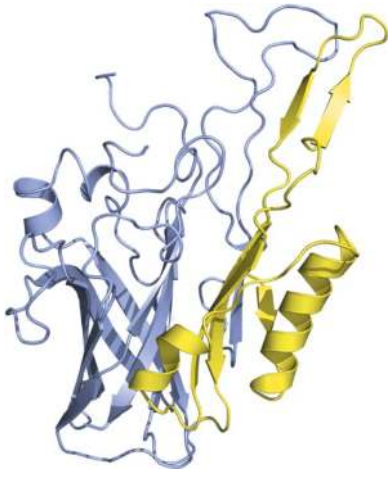

Table 1
Data-collection and refinement statistics.

Values in parentheses are for the highest resolution shell.

Data collection	
Wavelength (Å)	1.1159
Temperature (°C)	−173
Space group	$P2_1$
Unit-cell parameters (Å, °)	a = 59.9, b = 65.0, c = 83.4, β = 106.0
Resolution range (Å)	35.09–1.995 (2.07–2.0)
No. of unique reflections	43471
R_{meas}† (%)	6.8 (35.9)
Completeness (%)	99.2 (96.3)
$\langle I/\sigma(I)\rangle$	11.6 (3.3)
Multiplicity	3.5
Wilson B factor (Å^2)	28.87
Refinement	
R_{work}/R_{free} (%)	17.3/22.7
No. of protein molecules/non-H atoms	4722
No. of solvent atoms	374
Coordinate deviation	
R.m.s.d., bonds (Å)	0.008
R.m.s.d., angles (°)	1.11
Ramachandran plot	
Allowed (%)	98
Generously allowed (%)	2
Disallowed (%)	0
PDB code	4u9c

† $R_{meas} = \sum_{hkl}\{N(hkl)/[N(hkl)-1]\}^{1/2}\sum_i |I_i(hkl) - \langle I(hkl)\rangle|/\sum_{hkl}\sum_i I_i(hkl)$, where $I_i(hkl)$ is the ith observation of reflection hkl and $\langle I(hkl)\rangle$ is the weighted average intensity for all i observations of reflection hkl.

1999). Human transferrin and lactoferrin are highly similar in sequence (61.4% identical), have nearly identical folds and have a similar mechanism for iron binding (for a review, see Wally & Buchanan, 2007). Despite these similarities, the proteins exhibit different cellular functions and hence different iron-release properties. Transferrin binds to a cell receptor resulting in iron release within the endosome (pH 5–6). In contrast, lactoferrin will release iron at the acidic pH of 3–4 (Mazurier & Spik, 1980). While serum transferrin plays an important role in iron transport, the primary role of lactoferrin does not appear to be iron transport; rather, it acts as a component of the innate immune response (Caccavo *et al.*, 2002). The protein sequesters iron at mucosal surfaces, preventing bacterial growth. Lactoferrin also exhibits direct antimicrobial action following pepsin digestion of the N-terminus that releases a 49-amino-acid cationic peptide known as lactoferricin. This peptide exhibits a wide range of antimicrobial properties, killing bacteria and viruses (Gifford *et al.*, 2005).

The pathogen *Neisseria* has evolved a homologous two-component system to acquire iron from host transferrin and lactoferrin. The system consists of a membrane-bound transporter that extracts and transports iron across the outer membrane (called TbpA for transferrin and LbpA for lactoferrin), and a lipoprotein that delivers iron-loaded lactoferrin/transferrin to the transporter (called TbpB for transferrin and LbpB for lactoferrin). While a recent plethora of crystal structures of the transferrin-binding apparatus (TbpA and TbpB) has revealed many of the molecular details of how iron is extracted and transported from transferrin (Calmettes *et al.*, 2011, 2012; Moraes *et al.*, 2009; Noinaj, Buchanan *et al.*, 2012; Noinaj, Easley *et al.*, 2012), relatively little is known regarding how the LbpB and LbpA transport system interacts with lactoferrin. Here, we report the crystal structure of the N-lobe of LbpB from *N. meningitidis*. Docking the structure with lactoferrin reveals important clues regarding the function of LbpB in iron acquisition, and reveals a potential role for the protein in protecting the bacteria from the toxic effects of lactoferricin.

2. Materials and methods

2.1. Protein expression and purification

The sequences of full-length LbpB (residues 20–725; the 19-amino-acid membrane anchor was removed) and the N-terminal domain of LbpB (N-lobe; residues 20–346) were amplified from *N. meningitidis* strain MC58 and cloned into a previously described custom expression vector containing an N-terminal 6×His tag, maltose-binding protein (MBP) and a *Tobacco etch virus* (TEV) protease cleavage site (Arutyunova *et al.*, 2012). The constructs were transformed into *Escherichia coli* BL21 (DE3) cells and the proteins were induced with 0.1 m*M* IPTG and expressed at 22°C for 16 h. Cells were lysed at 103 MPa using an Emulsiflex C3 (Avestin, Canada), insoluble material was removed by centrifugation (27 000*g*, 25 min) and the supernatant was loaded onto an Ni–NTA column (ThermoFisher Scientific, USA). The protein was eluted with a 0–0.5 *M* imidazole gradient and the MBP tag was removed by incubating the protein sample with TEV protease [1:100(*w*:*w*) protease:protein] overnight at 4°C. The protein was concentrated and injected onto a Superdex 200 16/60 column (GE, Canada) pre-equilibrated with 20 m*M* Tris pH 8.0, 0.15 *M* NaCl. Both the full-length and the N-lobe of LbpB eluted as a single monodisperse peak and were subsequently used for crystallization screening.

2.2. Crystallization, data collection, structure determination and refinement

Purified full-length LbpB and LbpB N-lobe from *N. meningitidis* MC58 (15–20 mg ml^{-1}) were initially screened against The JCSG+ and PEGs Suites sparse-matrix screens (Qiagen, USA) using a 96-head Gryphon robot (Art Robbins Instruments, USA). Crystals of LbpB N-lobe measuring 0.2 × 0.2 × 0.2 mm were obtained using 0.1 *M* sodium acetate pH 4.6, 25% PEG 4000 at 25°C. Crystals of LbpB N-lobe were dipped in mother liquor supplemented with 30% glycerol and cooled in liquid nitrogen. X-ray data were collected at −173°C on beamline 8.3.1 at the Advanced Light Source (ALS; Berkeley, California, USA). The crystals diffracted to 2 Å resolution and crystallographic data were processed using *xia*2 (Winter *et al.*, 2013). The crystals belonged to the monoclinic space group $P2_1$ with two molecules per asymmetric unit (Table 1). The structure of LbpB N-lobe was determined by molecular replacement using *Phaser* (McCoy *et al.*, 2007) as implemented in *PHENIX* (Adams *et al.*, 2010) using the previously solved structure of the N-lobe domain of TbpB as a search model (PDB entry 3hoe; Moraes *et al.*, 2009). Refinement was carried out with *phenix.refine* including NCS restraints, TLS parameters, individual *B* factors, occupancies and the addition of riding H atoms (Adams *et al.*, 2010), and manual electron-density-map fitting was carried out using *Coot* (Emsley & Cowtan, 2004). The final refinement and model statistics are given in Table 1.

2.3. Docking of LbpB N-lobe with human lactoferrin

Blind docking of *N. meningitidis* LbpB N-lobe with the structure of human lactoferrin (pdb entry 1lfg; Haridas *et al.*, 1995) and *M. bovis* LbpB N-lobe (PDB entry 3uaq; Arutyunova *et al.*, 2012) with the structure of bovine lactoferrin (PDB entry 1blf; Moore *et al.*, 1997) was conducted using *ZDOCK* (Pierce *et al.*, 2014). The initially placed docked structures were then submitted to *RosettaDock* (Lyskov *et al.*, 2013) and the lowest energy models were examined.

3. Results and discussion

3.1. Structure of LbpB N-lobe and identification of the lactoferrin-binding site

Full-length LbpB and the N-terminal domain of the protein (N-lobe; residues 20–346) were expressed and purified for crystallization trials. Despite exhaustive crystal screening, no crystals of full-length LbpB were obtained. However, crystals of the N-lobe readily appeared and the structure was solved by molecular replacement using the structure of TbpB as a search model (Table 1; Moraes *et al.*, 2009). No electron density was apparent for the N-terminal 21 amino acids, indicating either disorder or loss of the region during purification. The structure of LbpB N-lobe exhibited the same global architecture as found in previously solved structures of LbpB N-lobe from *Moraxella bovis* and TbpB N-lobe from *Actinobacillus pleuropneumoniae*, *A. suis* and *N. meningitidis* (Noinaj, Easley *et al.*, 2012; Moraes *et al.*, 2009; Calmettes *et al.*, 2011, 2012; Arutyunova *et al.*, 2012). The structure consists of two domains: a handle domain (residues 41–171) and a β-barrel domain (residues 172–344) (Fig. 1*a*). Long loops project from both domains, forming an extended cap region 58 Å across and 42 Å wide. Based on the structure, a reasonable approximation of the lactoferrin-binding site can be made. Early work on LbpB hypothesized that a stretch of negatively charged amino acids in the C-terminal domain interacted with positively charged regions of lactoferrin (Pettersson *et al.*, 1998). However, recent work has shown that these charged regions are involved in protection against the antimicrobial effects of the lactoferrin-derived cationic peptide lactoferricin, and may not play a role in iron acquisition (Morgenthau *et al.*, 2014). The recent crystal structure of TbpB from *N. meningitidis* in complex with transferrin unequivocally identifies the cap region of the TbpB N-lobe as the interface site between the two proteins (Calmettes *et al.*, 2012). Given the high degree of structural similarity between TbpB and LbpB, this extended cap region of the N-lobe is likely to represent the lactoferrin-binding site (Fig. 1*a*).

The structure of LbpB from *M. bovis* has previously been determined (Arutyunova *et al.*, 2012) and the two LbpB structures show a large number of similarities. The amino-acid sequences of *N. meningitidis* and *M. bovis* LbpB are homologous, sharing 34% sequence identity. Given the level of sequence identity, it is no surprise that the two N-lobe structures are highly comparable (r.m.s.d. of 0.78 Å), with the core of the handle and β-barrel domains being nearly identical (Fig. 1*b*). The largest differences in the structures occur at the loop regions protruding from the handle domain. This results in the *N. meningitidis* N-lobe cap region being more extended than the *M. bovis* N-lobe structure (Fig. 1*b*). Differences between the structures are to be expected and are likely to be responsible for the important distinctions in LbpB specificity. LbpB is host-species restricted, with *M. bovis* LbpB binding only bovine lactoferrin and human LbpB binding only human lactoferrin (Yu & Schryvers, 2002; Arutyunova *et al.*, 2012).

3.2. The role of LbpB in iron acquisition from lactoferrin

To understand the role of LbpB in iron acquisition, it is important to dissect its interaction with lactoferrin. Biochemical evidence suggests subtle differences in how the lactoferrin- and transferrin-transport systems interact with their target proteins. Membrane preparations from *N. meningitidis*, *N. gonorrhoeae* and *M. catarrhalis* containing both LbpA and LbpB were found to bind both the N- and C-lobes of lactoferrin (Yu & Schryvers, 1993). A later study examining the specificity of LbpA alone found that only the lactoferrin C-lobe interacted with the protein (Wong & Schryvers, 2003). Therefore, it seems probable that the observed binding to the

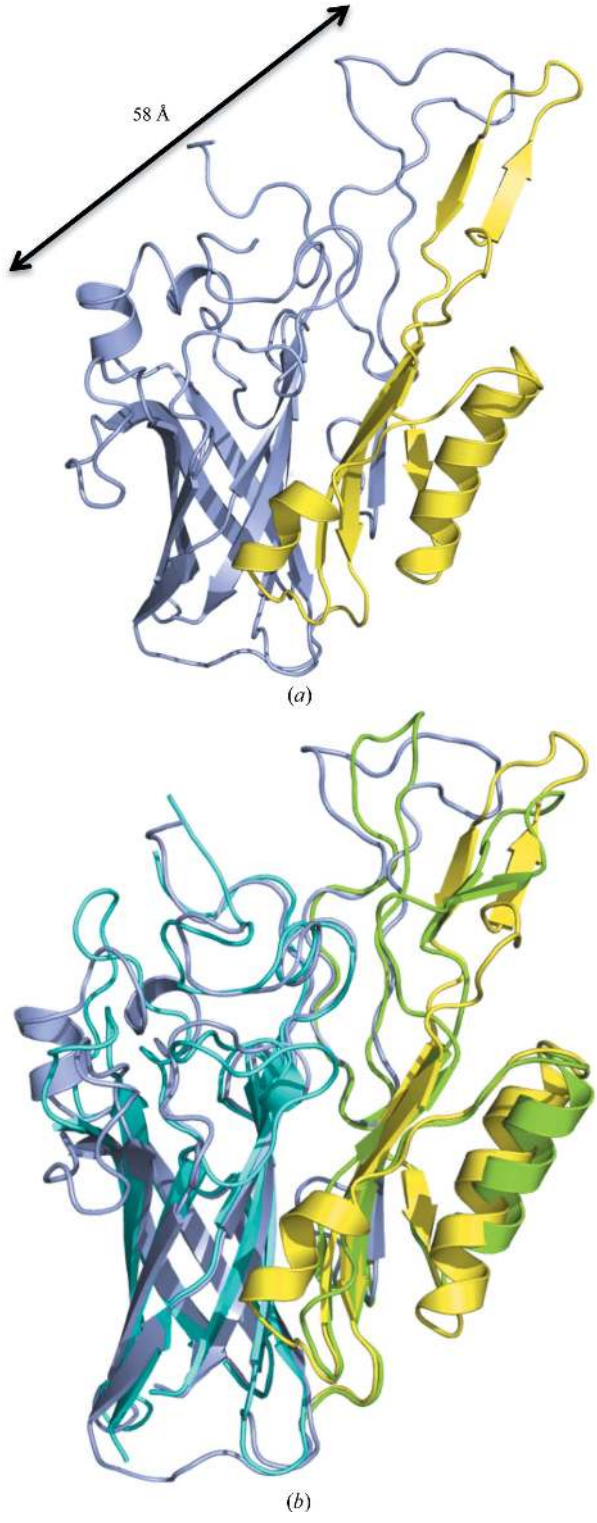

Figure 1
Crystal structure of the N-lobe of *N. meningitidis* LbpB. (*a*) The putative lactoferrin-binding site is located in the cap region (top), which is 58 Å on the long edge. The binding site is formed at the interface of the two LbpB subdomains: the handle domain (yellow) and the β-barrel domain (purple). (*b*) Structural alignment of *N. meningitidis* LbpB (purple and yellow) and *M. bovis* LbpB (the β-barrel domain is shown in aqua and the handle domain is shown in green; r.m.s.d. of 0.78 Å).

lactoferrin N-lobe may come from LbpB. In the transferrin-binding system, it has been established that the N-lobe of TbpB binds transferrin (Alcantara *et al.*, 1993; Calmettes *et al.*, 2012; Retzer *et al.*, 1999). Given the high degree of structural similarity between TbpB and LbpB, it is reasonable to conclude that the N-lobe of LbpB must bind lactoferrin. Blind docking of LbpB with human lactoferrin returned similar binding models, all of which showed the N-lobe of lactoferrin binding to the N-lobe of *N. meningitidis* LbpB in agreement with the above biochemical data.

The initial docked model was then further refined using *Rosetta* (Lyskov *et al.*, 2013) and the lowest energy model was used for subsequent analysis (Fig. 2*a*). The handle domain of LbpB N-lobe interacts extensively with the α/β N1 subdomain of lactoferrin, while loops extending from the β-barrel domain of LbpB interact with loops protruding from both the N1 and N2 lactoferrin subdomains. The blind docking studies also revealed subtle differences between the LbpB N-lobes from *N. meningitidis* and *M. bovis* in complex with lactoferrin (Fig. 2*b*). The N1 subdomain of bovine lactoferrin was predicted to interact with the LbpB handle domain, and loops from the lactoferrin N2 subdomain to interact with loops from the LbpB β-barrel.

The predicted binding models of LbpB with lactoferrin (Figs. 2*a* and 2*b*) provide important clues regarding the function of LbpB in host iron acquisition and transport. TbpB plays a dual role in iron acquisition. TbpB has absolute specificity for hololactoferrin and thus ensures delivery of iron-loaded transferrin to TbpA. This is important as TbpA cannot distinguish between apotransferrin and holotransferrin (Cornelissen & Sparling, 1996; Retzer *et al.*, 1998). The recent crystal structure of TbpB in complex with human transferrin also points to a role for the protein in stabilizing the holo form of transferrin by preventing discharge of iron prior to interaction with the TbpA transporter (Calmettes *et al.*, 2012). LbpB may be playing a similar role in ensuring that hololactoferrin is delivered to LbpA, albeit by a different mechanism. Transferrin contains residues that respond to changing pH, facilitating iron release (He *et al.*, 1999; Steere *et al.*, 2010). TbpB stabilizes the transferrin holo form by protonating His349, which prevents the conformational change required for iron release (Calmettes *et al.*, 2012). In contrast, lactoferrin has no such pH-sensitive residues, and retains iron even at very low pH. Thus, LbpB is unlikely to have a role in directly stabilizing the holo form of lactoferrin, but rather provides specificity to the iron-transport system. Large structural changes are associated with the transition from hololactoferrin to apolactoferrin. In the absence of iron, the N1 and N2 subdomains of lactoferrin rotate away from each other by 54°, opening up the iron-binding cleft (Fig. 2*c*;

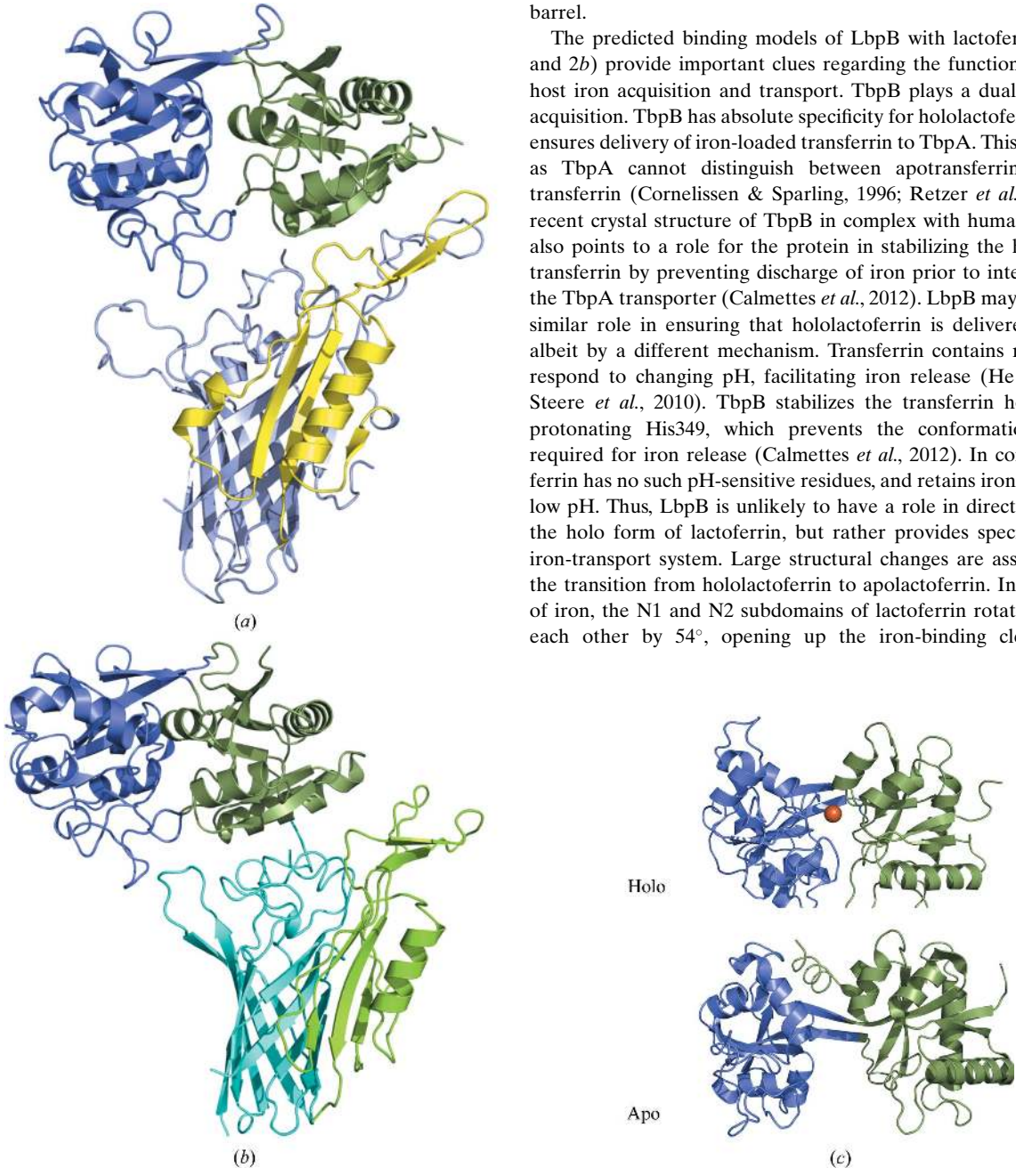

Figure 2
Docking of lactoferrin with LbpB. (*a*) Interaction of human lactoferrin N-lobe with *N. meningitidis* LbpB N-lobe. The LbpB handle domain (yellow) and loops from the barrel domain (blue) interact with the lactoferrin N1 subdomain (green). The N2 subdomain of lactoferrin (slate) binds primarily to the barrel domain of LbpB (blue). (*b*) Binding of bovine lactoferrin to *M. bovis* LbpB. The LbpB handle domain (bright green) and loops from the barrel domain (cyan) interact with the lactoferrin N1 subdomain (green). The N2 subdomain of lactoferrin (slate) binds primarily to the barrel domain of LbpB (cyan). (*c*) Lactoferrin undergoes large structural changes upon iron binding. The holo structure (top) is in a closed conformation (iron is shown as an orange sphere); upon iron release a large rotation between the N1 (green) and N2 (slate) subdomains occurs (bottom). This large change in the apo structure would preclude LbpB binding.

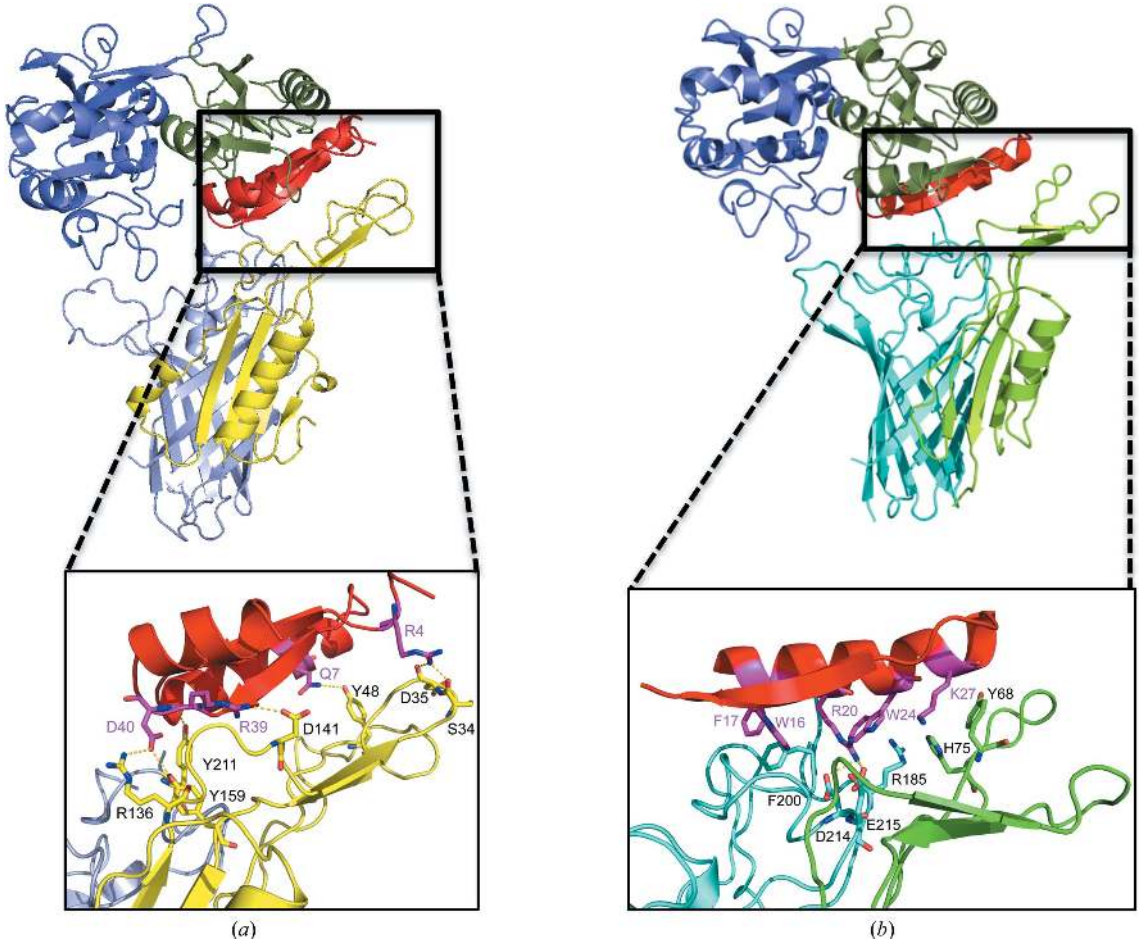

Figure 3
Interaction of LbpB with lactoferricin. (*a*) Interaction of human lactoferricin (red) with LbpB from *N. meningitidis*. Interactions are mediated by hydrogen bonds and salt bridges (yellow dashes). (*b*) Interaction of bovine lactoferricin (red) with LbpB from *M. bovis*. Interactions are mediated by hydrophobic stacking and a single salt bridge (yellow dashes).

Anderson *et al.*, 1990). This open apolactoferrin conformation would be incompatible with LbpB binding, as both the N1 and N2 subdomains are involved in the binding interaction (Figs. 2*a* and 2*b*). Similar to TbpB, by exhibiting specificity for hololactoferrin, LbpB ensures that iron-loaded lactoferrin is delivered to LbpA, which extracts iron from lactoferrin for transport and use by the bacteria.

3.3. Role of LbpB N-lobe in neutralization of lactoferricin

Analysis of the binding model also points to a potential secondary role for LbpB in protection of *N. meningitidis* from the toxic effects of the cationic peptide lactoferricin. One of the principal differences between lactoferrin and transferrin is the positively charged N-terminal region of lactoferrin. Pepsin digestion of this charged region releases N-terminal fragments that exhibit a wide range of antimicrobial activity (Gifford *et al.*, 2005). In many species the C-terminal domain of LbpB (C-lobe) contains stretches of negatively charged residues (Adamiak *et al.*, 2012). These regions help to protect *Neisseria* against the toxic effects of the lactoferricin peptide by binding and neutralizing the peptide (Morgenthau *et al.*, 2012, 2014). Our docked structural models point to an additional role of the LbpB N-lobe in protection against lactoferricin. Lactoferricin is situated in the N1 subdomain of lactoferrin, with human lactoferricin comprising the first 49 N-terminal residues of lactoferrin, while bovine lactoferricin comprises residues 17–41 (Bellamy *et al.*, 1992). Both docked models of *M. bovis* and *N. meningitidis* LbpB N-lobes predict interactions between LbpB and the region of the lactoferricin peptide (Figs. 3*a* and 3*b*). In the case of *N. meningitidis* LbpB a series of hydrogen bonds and salt bridges extending from the handle domain interact with human lactoferricin (Fig. 3*a*). A slightly different interaction pattern is observed with *M. bovis* LbpB, where a series of hydrophobic packing interactions surround a single key salt bridge that stabilizes the centre of the complex (Fig. 3*b*). LbpB binding to the N1 lactoferrin subdomain could act to shelter lactoferrin from pepsin digestion. This may prevent the subsequent release of the toxic lactoferricin peptide, hence protecting the invading bacteria from the antimicrobial properties of the protein. Alternatively, the N-lobe may bind free lactoferricin, providing a second route of peptide sequestration by LbpB. This may be especially important for *M. bovis* as LbpB from this species lacks the negatively charged region in the C-lobe (Adamiak *et al.*, 2012).

4. Conclusion

The structure of the LbpB N-lobe from *N. meningitidis* has unveiled several surprising facets of how *Neisseria* obtains iron from its host and neutralizes the antimicrobial properties of lactoferrin. Despite a high degree of structural homology and functional similarities to TbpB, there are important differences. LbpB binds the N-lobe of

lactoferrin, whereas TbpB binds the C-lobe of transferrin. Both proteins provide specificity for iron-loaded protein, with TbpB stabilizing the holo form of transferrin by the manipulation of pH-sensitive residues and LbpB stabilizing the holo form of lactoferrin by binding the N1 and N2 subdomains, preventing conformational changes that release iron. This binding interface also provides specificity for the holo form of the protein, as the open conformation of lactoferrin would be unable to bind LbpB. Unlike TbpB, the N-lobe of LbpB may also have a role in protecting the bacteria from the antimicrobial peptide lactoferricin. Our structure points to a novel mechanism of lactoferricin neutralization in which the N-terminal region of lactoferrin that generates the lactoferricin peptide binds LbpB. This may prevent proteolysis of lactoferrin or it may be able to bind the free peptide, neutralizing the toxic effects. Future work will focus on uncovering biological and biochemical evidence for the multifaceted roles of LbpB in *Neisseria* infection.

X-ray data were collected at the Advanced Light Source (ALS), Berkeley, California, USA. We thank Dr Anthony Schryvers at the University of Calgary for the LbpB expression plasmids. MJL is supported by grants from the Alberta Heritage Foundation for Medical Research and Womens and Children's Health Research Institute (WCHRI). MJL is Canada Research Chair in Membrane Protein Structure and Function, and an Alberta Innovates Health Solutions Scientist. CLB is supported by start-up funds from CSU-Fresno and a CSUPERB new investigator grant.

References

Adamiak, P., Beddek, A. J., Pajon, R. & Schryvers, A. B. (2012). *Biochem. Cell Biol.* **90**, 339–350.

Adams, P. D. *et al.* (2010). *Acta Cryst.* D**66**, 213–221.

Ala'Aldeen, D. A. & Borriello, S. P. (1996). *Vaccine*, **14**, 49–53.

Ala'Aldeen, D. A., Stevenson, P., Griffiths, E., Gorringe, A. R., Irons, L. I., Robinson, A., Hyde, S. & Borriello, S. P. (1994). *Infect. Immun.* **62**, 2984–2990.

Alcantara, J., Yu, R. H. & Schryvers, A. B. (1993). *Mol. Microbiol.* **8**, 1135–1143.

Anderson, B. F., Baker, H. M., Morris, G. E., Rumball, S. V. & Baker, E. N. (1990). *Nature (London)*, **344**, 784–787.

Archibald, F. S. & DeVoe, I. W. (1978). *J. Bacteriol.* **136**, 35–48.

Arutyunova, E., Brooks, C. L., Beddek, A., Mak, M. W., Schryvers, A. B. & Lemieux, M. J. (2012). *Biochem. Cell Biol.* **90**, 351–361.

Bellamy, W., Takase, M., Yamauchi, K., Wakabayashi, H., Kawase, K. & Tomita, M. (1992). *Biochim. Biophys. Acta*, **1121**, 130–136.

Caccavo, D., Pellegrino, N. M., Altamura, M., Rigon, A., Amati, L., Amoroso, A. & Jirillo, E. (2002). *J. Endotoxin Res.* **8**, 403–417.

Calmettes, C., Alcantara, J., Yu, R. H., Schryvers, A. B. & Moraes, T. F. (2012). *Nature Struct. Mol. Biol.* **19**, 358–360.

Calmettes, C., Yu, R.-H., Silva, L. P., Curran, D., Schriemer, D. C., Schryvers, A. B. & Moraes, T. F. (2011). *J. Biol. Chem.* **286**, 12683–12692.

Cornelissen, C. N. & Sparling, P. F. (1996). *J. Bacteriol.* **178**, 1437–1444.

Emsley, P. & Cowtan, K. (2004). *Acta Cryst.* D**60**, 2126–2132.

Gifford, J. L., Hunter, H. N. & Vogel, H. J. (2005). *Cell. Mol. Life Sci.* **62**, 2588–2598.

Haridas, M., Anderson, B. F. & Baker, E. N. (1995). *Acta Cryst.* D**51**, 629–646.

He, Q.-Y., Mason, A. B., Tam, B. M., MacGillivray, R. T. & Woodworth, R. C. (1999). *Biochemistry*, **38**, 9704–9711.

Lissolo, L., Maitre-Wilmotte, G., Dumas, P., Mignon, M., Danve, B. & Quentin-Millet, M.-J. (1995). *Infect. Immun.* **63**, 884–890.

Lyskov, S. *et al.* (2013). *PLoS One*, **8**, e63906.

Mazurier, J. & Spik, G. (1980). *Biochim. Biophys. Acta*, **629**, 399–408.

McCoy, A. J., Grosse-Kunstleve, R. W., Adams, P. D., Winn, M. D., Storoni, L. C. & Read, R. J. (2007). *J. Appl. Cryst.* **40**, 658–674.

Moore, S. A., Anderson, B. F., Groom, C. R., Haridas, M. & Baker, E. N. (1997). *J. Mol. Biol.* **274**, 222–236.

Moraes, T. F., Yu, R.-H., Strynadka, N. C. & Schryvers, A. B. (2009). *Mol. Cell*, **35**, 523–533.

Morgenthau, A., Beddek, A. & Schryvers, A. B. (2014). *PLoS One*, **9**, e86243.

Morgenthau, A., Livingstone, M., Adamiak, P. & Schryvers, A. B. (2012). *Biochem. Cell Biol.* **90**, 417–423.

Noinaj, N., Buchanan, S. K. & Cornelissen, C. N. (2012). *Mol. Microbiol.* **86**, 246–257.

Noinaj, N., Easley, N. C., Oke, M., Mizuno, N., Gumbart, J., Boura, E., Steere, A. N., Zak, O., Aisen, P., Tajkhorshid, E., Evans, R. W., Gorringe, A. R., Mason, A. B., Steven, A. C. & Buchanan, S. K. (2012). *Nature (London)*, **483**, 53–58.

Pettersson, A., Kortekaas, J., Weynants, V. E., Voet, P., Poolman, J. T., Bos, M. P. & Tommassen, J. (2006). *Vaccine*, **24**, 3545–3557.

Pettersson, A., Prinz, T., Umar, A., van der Biezen, J. & Tommassen, J. (1998). *Mol. Microbiol.* **27**, 599–610.

Pierce, B. G., Wiehe, K., Hwang, H., Kim, B.-H., Vreven, T. & Weng, Z. (2014). *Bioinformatics*, **30**, 1771–1773.

Retzer, M. D., Yu, R.-H. & Schryvers, A. B. (1999). *Mol. Microbiol.* **32**, 111–121.

Retzer, M. D., Yu, R.-H, Zhang, Y., Gonzalez, G. C. & Schryvers, A. B. (1998). *Microb. Pathog.* **25**, 175–180.

Rokbi, B., Mignon, M., Maitre-Wilmotte, G., Lissolo, L., Danve, B., Caugant, D. A. & Quentin-Millet, M.-J. (1997). *Infect. Immun.* **65**, 55–63.

Rokbi, B., Renauld-Mongenie, G., Mignon, M., Danve, B., Poncet, D., Chabanel, C., Caugant, D. A. & Quentin-Millet, M. J. (2000). *Infect. Immun.* **68**, 4938–4947.

Schryvers, A. B. & Stojiljkovic, I. (1999). *Mol. Microbiol.* **32**, 1117–1123.

Steere, A. N., Byrne, S. L., Chasteen, N. D., Smith, V. C., MacGillivray, R. T. & Mason, A. B. (2010). *J. Biol. Inorg. Chem.* **15**, 1341–1352.

Wally, J. & Buchanan, S. K. (2007). *Biometals*, **20**, 249–262.

Weinberg, E. D. (2009). *Biochim. Biophys. Acta*, **1790**, 600–605.

Winter, G., Lobley, C. M. C. & Prince, S. M. (2013). *Acta Cryst.* D**69**, 1260–1273.

Wong, H. & Schryvers, A. B. (2003). *Microbiology*, **149**, 1729–1737.

Yu, R.-H. & Schryvers, A. B. (1993). *Microb. Pathog.* **14**, 343–353.

Yu, R.-H. & Schryvers, A. B. (2002). *Biochem. Cell Biol.* **80**, 81–90.